Biogeosciences Discuss., 12, 7301–7333, 2015
www.biogeosciences-discuss.net/12/7301/2015/
doi:10.5194/bgd-12-7301-2015

Biogeosciences Discussions
Open Access

Colored dissolved organic matter in shallow estuaries: the effect of source on quantification

W. K. Oestreich[1], N. K. Ganju[2], J. W. Pohlman[2], and S. E. Suttles[2]

[1]Department of Civil & Environmental Engineering, Northwestern University, Evanston, IL, USA
[2]US Geological Survey Woods Hole Coastal and Marine Science Center, Woods Hole, MA, USA

Received: 17 April 2015 – Accepted: 21 April 2015 – Published: 18 May 2015

Correspondence to: N. K. Ganju (nganju@usgs.gov)

Published by Copernicus Publications on behalf of the European Geosciences Union.

Abstract

Light availability is of primary importance to the ecological function of shallow estuaries. For example, benthic primary production by submerged aquatic vegetation is contingent upon light penetration to the seabed. A major component that attenuates light in estuaries is colored dissolved organic matter (CDOM). CDOM is often measured via a proxy, fluorescing dissolved organic matter (fDOM), due to the ease of in situ fDOM measurements. Fluorescence must be converted to CDOM absorbance for use in light attenuation calculations and models. However, this fDOM-CDOM relationship varies among and within estuaries. We quantified the variability in this relationship within three estuaries: West Falmouth Harbor (MA), Barnegat Bay (NJ), and Chincoteague Bay (MD, VA). Land use surrounding these estuaries ranges from urban to developed, with varying sources of nutrients and organic matter. Measurements of fDOM and CDOM absorbance were taken along a terrestrial-to-marine gradient in all three estuaries. The ratio of the absorption coefficient at 340 nm (m^{-1}) to fDOM (QSU) was higher in West Falmouth Harbor (1.22) than in Barnegat Bay (0.22) and Chincoteague Bay (0.17). The fDOM-CDOM absorption ratio was variable between sites within West Falmouth Harbor and Barnegat Bay, but consistent between sites within Chincoteague Bay. Stable carbon isotope analysis for constraining the source of dissolved organic matter in West Falmouth Harbor and Barnegat Bay yielded $\delta^{13}C$ values ranging from −19.7 to −26.1 ‰ and −20.8 to −26.7 ‰, respectively. Stable carbon isotope mixing models of DOC in the estuaries indicate contributions from marine plankton, terrestrial plants, and *Spartina* cordgrass. Comparison of DOC source to fDOM-CDOM absorption ratio at each site demonstrates the influence of source on optical properties. Samples with a greater contribution from marsh (*Spartina*) organic material had higher fDOM-CDOM absorption ratios than samples with greater contribution from terrestrial organic material. Applying a uniform fDOM-CDOM absorption ratio and spectral slope within a given estuary yields errors in modeled light attenuation ranging from 11–33 % depending on estuary. The application of a uniform absorption ratio across all estuaries doubles this

BGD
12, 7301–7333, 2015

error. These results demonstrate that continuous monitoring of light attenuation in estuaries requires some quantification of CDOM absorption and source to refine light models.

1 Introduction

Benthic primary production in estuaries, including those along the Atlantic coast of the United States, is typically dominated by seagrass (Heck et al., 1995). Furthermore, seagrass acts as an ecosystem engineer in temperate coastal ecosystems via habitat provision and nutrient cycling (Ehlers et al., 2008). Recent anthropogenic nutrient loading to these ecosystems due to industrial and agricultural development has caused a loss of seagrass density. This occurs as eutrophication creates water column algal blooms and increases benthic algae populations (Burkholder et al., 2007; Hauxwell et al., 2003). These algal processes reduce penetration of the light necessary for survival of seagrasses. As anthropogenic impacts on coastal ecosystems compound with increasing urbanization of coastal zones (McGranahan et al., 2007), it is important to understand the factors controlling light attenuation in the estuarine water column.

Four main factors attenuate light in the water column: water itself, non-algal particulate material, phytoplankton, and colored dissolved organic matter (CDOM) (Kirk, 1994). Proxies are typically used to quantify these factors in situ: depth, turbidity, chlorophyll *a* fluorescence, and fluorescing dissolved organic matter (fDOM), respectively (Ganju et al., 2014). The use of fDOM as a proxy for the CDOM component is widespread due to the ease of measuring in situ fluorescence, and the relationship between fDOM and CDOM absorbance. However, considerable variability in the fDOM-CDOM absorption ratios has been observed both between and within numerous aquatic systems (Hoge et al., 1993; Del Castillo et al., 1999; Clark et al., 2004). Quantifying and understanding the variability in this relationship is required to accurately model light attenuation and seagrass viability in estuaries.

BGD
12, 7301–7333, 2015

Estuaries are transition zones between freshwater and marine systems where dissolved organic carbon from a variety of sources mixes (Raymond and Bauer, 2001). The major sources of DOC to estuaries are typically terrestrial DOC from riverine inputs, oceanic DOC from phytoplankton, and tidal marsh DOC from *Spartina* spp. (Peterson et al., 1994). Marine and terrestrial DOM exhibit different structural characteristics (Harvey et al., 1983) that are reflected in the optical properties of CDOM (Helms et al., 2008; De Souza Sierra et al., 1994). Due to its role in attenuating light in the water column, measurement of CDOM and enhanced understanding of its source-dependent optical properties is important for modeling light availability in estuaries.

The goal of this study is to improve understanding of light attenuation in the estuarine water column by characterizing the optical properties and sources of CDOM in three diverse estuaries: West Falmouth Harbor (MA), Barnegat Bay (NJ), and Chincoteague Bay (MD, VA). Our objectives are to quantify the fDOM-CDOM absorption ratio, establish absorption spectral slopes for use in light models (Gallegos et al., 2011), determine the sources of CDOM in these estuaries, and identify variation in the fDOM-CDOM absorption ratio as a function of source.

2 Site descriptions

2.1 West Falmouth Harbor

West Falmouth Harbor is a small (0.7 km^2), groundwater-fed estuary on the western shore of Cape Cod, Massachusetts (Fig. 1b). The harbor has a mean depth of approximately 1 m, and is connected to Buzzard's Bay (and ultimately the Atlantic Ocean) by a 3 m deep, 150 m wide channel. Residence time in the harbor is approximately one day (Hayn et al., 2014). Tide range is 1.9 m during spring tides and 0.7 m during neap tides, with tidal currents at the mouth approaching 0.5 $m\,s^{-1}$. The dominant source of freshwater and nutrients is groundwater. Land use surrounding the harbor is largely residential, with influence from a legacy wastewater plume within the aquifer

BGD
12, 7301–7333, 2015

(Ganju et al., 2012). Plant coverage in surrounding wetlands is variable, but *Spartina alterniflora* and *Spartina patens* tend to dominate, with some lesser coverage by *Juncus gerardi* and forbs such as *Salicornia* spp., *Limonium carolinianum*, and *Solidago sempervirens* (Buchsbaum and Valiela, 1987).

2.2 Barnegat Bay

The Barnegat Bay–Little Egg Harbor estuary is a back-barrier system along the New Jersey Atlantic coast (Fig. 1c). The estuary is approximately 70 km long, 2–6 km wide, and 1.5 m deep. Bay and ocean water exchange occurs at three inlets: the Point Pleasant Canal at the northern limit, Barnegat Inlet in the middle of the barrier island, and Little Egg Inlet at the southern limit. Limited exchange through these inlets leads to a spatially variable residence time exceeding 30 d in some locations (Defne and Ganju, 2014). For the purpose of this study, sites north of Barnegat Inlet are referred to as "North Barnegat Bay", while sites parallel to and south of Barnegat Inlet are referred to as "South Barnegat Bay." Tides are semidiurnal and range from < 0.1–1.5 m, and current velocities range from < 0.5–1.5 m s^{-1} (Kennish et al., 2013; Ganju et al., 2014); there is also a pronounced south-to-north gradient in tidal range and flushing (Defne and Ganju, 2014). While the land surrounding the northern portion of the bay is developed with mixed urban-residential land use, the area south of Barnegat Inlet is less developed and retains much of the original marsh (Wieben and Baker, 2009). The salt marshes south of Barnegat Inlet are dominated by *Spartina alterniflora* (Olsen and Mahoney, 2001). Freshwater inputs are largest at the northern end of the bay due to the Toms River, Metedeconk River, and Cedar Creek (US EPA, 2007).

2.3 Chincoteague Bay

Chincoteague Bay is along the Atlantic coast of the Delmarva Peninsula (Fig. 1d). This estuary has an area of 355 km^2 and an average depth of 2 m. The watershed surrounding Chincoteague Bay is 487 km^2, and consists of 31 % agricultural development, 25 %

BGD
12, 7301–7333, 2015

wetlands, and 8 % urban development (Bricker et al., 1999). Vegetation in the wetland portion is dominated by *Spartina alterniflora*, much like South Barnegat Bay (Keefe and Boynton, 1973). Tide range averages 0.5 m, and residence time has been estimated at 8 d (Bricker et al., 1999). The Bay is connected to the ocean via two inlets: Ocean City Inlet in the north and Chincoteague Inlet in the south (Allen et al., 2007). Historically, Chincoteague Bay has been marked by extensive seagrass coverage and higher water quality, especially compared to other more developed and less well-flushed bays on the Atlantic coast (Wazniak et al., 2004).

3 Methods

3.1 Fluorescence measurements

Sampling sites were approached by both land (WF01–WF13, BB01–BB07) and sea (BB08–BB16, CB01–CB10). Sampling occurred from 25 June to 17 July 2014 (Table 1). Either a bucket (sites approached on foot) or one-liter Nalgene sampling bottle (sites approached by boat) was rinsed with native water and then used to collect a surface water sample. A pre-calibrated YSI EXO 2 multisonde, measuring fDOM, temperature, salinity, pH, turbidity, chlorophyll *a* fluorescence, blue-green algae fluorescence, and dissolved oxygen concentration was placed in each sample. Excitation and emission wavelengths for the fluorescing dissolved organic matter sensor were 365 (±5 nm) and 460 (±40 nm), respectively. Measurements of each parameter were collected at 1 s intervals for approximately 60 s and averaged. For sites approached on foot, the YSI EXO was deployed immediately; for sites approached by boat, the YSI EXO was deployed later on land (in concurrence with absorbance measurements, as described below).

Temperature, turbidity, and inner filter effects (IFE) have been shown to alter fluorescence measurements (Baker, 2005; Downing et al., 2012). For this reason, we corrected fluorescence measurements to account for temperature, turbidity, and IFE, according to Downing et al. (2012).

BGD
12, 7301–7333, 2015

3.2 Absorbance measurements

A 60 ml syringe was used to draw a water sample from these buckets for absorbance measurements. Fifteen ml of this sample was filtered through a 0.2 µm inorganic membrane filter into a 5 cm path length cuvette. Absorbance measurements were recorded in 20-nm increments over the range of 340–440 nm (West Falmouth Harbor) or 340–720 nm (Barnegat Bay and Chincoteague Bay). All measurements were referenced against Milli-Q water, which was used as a blank. The estimated photometric accuracy of the spectrophotometer was 0.003 absorbance units. Absorbance measurements at each wavelength were converted to absorption coefficients as follows:

$$a(\lambda) = 2.303A(\lambda)/l \quad (1)$$

where $A(\lambda)$ is the absorbance at 340 nm, l is the cell length in meters (0.05 m for this study), and $a(\lambda)$ is the absorption coefficient (Green and Blough, 1994). 340 nm had the highest absorbance values across the range scanned and therefore was chosen as the absorbance wavelength for calculating the absorbance coefficient. Spectral slopes were calculated by plotting the natural log of absorption coefficient against wavelength. Due to use of the natural log, non-positive absorption coefficients were discarded to calculate spectral slope, as described in Eq. (2) (Bricaud et al., 1981):

$$S = \ln(a(\lambda)/a(r))(r - \lambda) \quad (2)$$

where λ is wavelength, r is a reference wavelength, $a(\lambda)$ is absorption coefficient at a given wavelength, $a(r)$ is absorption coefficient at the reference wavelength, and S is the spectral slope. The value of S shows the rate at which absorption decreases with increasing wavelength (Green and Blough, 1994). This parameter can be used to predict absorption coefficients across the spectrum based on absorption at one reference wavelength (Bricaud et al., 1981).

BGD
12, 7301–7333, 2015

3.3 Isotope analysis

At each site in West Falmouth Harbor and Barnegat Bay, water samples were collected for stable carbon isotope analysis of DOC (Chincoteague Bay was excluded due to logistical limitations). Following absorbance measurements, 30 mL of the collected sample was filtered through a 0.2 µm inorganic membrane filter, collected in a 40-ml glass autosampler vial that had been baked at 450 °C for 4 h and sealed with caps and Teflon-faced silicon septa that had been soaked and rinsed with 10 % (by volume) HCl. Additionally, trace metal grade 12N HCl (Sigma Aldrich) was added to each isotope water sample to achieve pH < 2. The vials were then stored at 4 °C. Samples were analyzed by High Temperature Combustion-Isotope Ratio Mass Spectrometry (HTC-IRMS) at the USGS-WHOI Dissolved Carbon Isotope Lab (DCIL), as described by Lalonde et al. (2014). The stable carbon isotope ratios are reported in the standard δ-notation relative to Vienna Pee Dee Belemnite (VPDB) and are corrected by mass balance to account for the analytical blank, which was less than the equivalent of 15 µM DOC in the sample. By comparison, the sample DOC concentrations ranged from 60.7 to 581 µM. Thus the blank correction was always less than 25 % of the sample concentration. The analytical precision of the δ^{13}C analysis was less than 0.3 ‰.

Salinity and δ^{13}C values for freshwater and marine endmembers from West Falmouth Harbor and Barnegat Bay were used to construct isotope mixing models for the estuaries (Kaldy et al., 2005). Marine and freshwater end-members are defined as the most and least saline samples collected at each estuary. Because of the number of samples clustered near the highest salinity for each estuary, marine end-members were checked with geographic location. For West Falmouth Harbor, the site chosen as marine end-member (WF01) was taken from the mouth of the harbor where the estuary connects to Buzzard's Bay. For Barnegat Bay, the site of highest salinity (BB13) was taken from the middle of Little Egg Harbor in South Barnegat Bay. However, a more geographically intuitive marine end-member would be site BB16, near Little Egg Inlet. The only slightly lower salinity at this site (29.69 psu) as compared to BB13 (30.08 psu),

BGD
12, 7301–7333, 2015

along with the geographic location of BB16 at an oceanic inlet, makes BB16 a more appropriate marine end-member. Therefore, end-members used in the conservative mixing models were as follows: WF06 (freshwater), WF01 (marine), BB01 (freshwater), and BB16 (marine). The conservative mixing models (Kaldy et al., 2005) were constructed as:

$$C_{\text{mix}} = fC_R + (1 - f)C_O \quad (3)$$

where C_{mix} is the calculated concentration for use in the mixing model, C_R and C_O are freshwater and marine end-member DOC concentrations, respectively, and f is the fraction of freshwater calculated from salinity:

$$f = (S_O - S_{\text{M}})/(S_O - S_R) \quad (4)$$

where S_{M} is measured salinity at a specific site, and S_R and S_O are freshwater and marine end-member salinities, respectively. These calculations lead to the modeled isotope ratio of each sample as:

$$\delta_{\text{mix}} = [fC_R\delta_R + (1 - f)C_O\delta_O]/C_{\text{mix}} \quad (5)$$

where all subscripts and variables are the same as described for Eqs. (3) and (4).

4 Results

4.1 Spectral slopes

The estuary-wide average spectral slope for West Falmouth was higher than for Barnegat and Chincoteague, with S_{avg} equal to 0.021, 0.013, and 0.014, respectively (Table 2). At West Falmouth Harbor, spectral slope ranged from 0.013–0.044, with a SD of 0.010. At Barnegat Bay, S ranged from 0.010–0.018, with a SD of 0.002. At Chincoteague Bay, S ranged from 0.006–0.020, with a SD of 0.004. All values observed for spectral slope were within ranges reported for similar estuaries and coastal waters (Keith et al., 2002; Green and Blough, 1994).

BGD
12, 7301–7333, 2015

4.2 Fluorescence measurements (fDOM)

At West Falmouth, fDOM ranged from 0.63–10.21 QSU, with a SD of 2.57 QSU. At Barnegat Bay, fDOM ranged from 12.06–84.40 QSU, with a SD of 20.82 QSU. At Chincoteague Bay, fDOM ranged from 11.15–49.49 QSU, with a SD of 10.95 QSU. Values observed for fDOM were within ranges reported for similar estuaries and coastal waters (Callahan et al., 2004; Clark et al., 2002; Green and Blough, 1994). Sites at West Falmouth and Barnegat Bay represented a freshwater to seawater gradient, with salinity ranging from 0.13–31.28 psu at West Falmouth and 3.41–30.08 psu at Barnegat. At Chincoteague Bay, salinity ranged from 25.88–31.85 psu. A complete salinity gradient was not sampled at Chincoteague due to the relatively high salinity found throughout the main basin of the bay, and low freshwater input. fDOM correlated inversely with salinity (Fig. 2), as expected because riverine input is typically the main external source of DOM. However, the slope and strength of the fDOM–salinity relationship differed both between and within estuaries. The strongest relationship was observed at Chincoteague Bay and in South Barnegat Bay. These two areas displayed a similar fDOM–salinity relationship, fDOM and salinity showed a slightly less negative relationship at South Barnegat Bay, and even less negative at West Falmouth Harbor.

4.3 CDOM absorption and fDOM-CDOM ratios

At West Falmouth, $a(340)$ ranged from 0.92–5.07 m^{-1}, with a SD of 1.02 m^{-1}. At Barnegat Bay, $a(340)$ ranged from 0.97–14.97 m^{-1}, with a SD of 3.99 m^{-1}. At Chincoteague Bay, $a(340)$ ranged from 1.84–8.38 m^{-1}, with a SD of 1.86 m^{-1} (Table 2). Absorption coefficients for West Falmouth and Chincoteague were comparable to those reported for similar estuaries and coastal waters (Chen et al., 2003; Green and Blough, 1994); absorption coefficients for Barnegat Bay were somewhat higher, but within the range reported by Green and Blough (1994). The ratio between $a(340)$ and fDOM differed both between and within estuaries, as expected (Table 2; Fig. 3). The mean ratio of $a(340)$ to fDOM was relatively higher in West Falmouth Harbor (1.22) than in

BGD
12, 7301–7333, 2015

Barnegat Bay (0.22) and Chincoteague Bay (0.17). There were two significant outliers at Barnegat Bay: BB01, which had a lower absorption coefficient (0.97 m^{-1}) than expected based on its higher fDOM value (69.92 QSU); and BB15, which showed a much higher absorption coefficient (14.97 m^{-1}) than expected based on its lower fDOM value (16.50 QSU). West Falmouth also demonstrated substantial variability in $a(340)$/fDOM ratio between sites. Chincoteague Bay however, showed a highly consistent ratio.

4.4 Stable carbon isotope analysis

The observed isotope–salinity relationship at West Falmouth Harbor and Barnegat Bay had numerous $\delta^{13}C$ values well outside the range predicted by the conservative mixing models (Table 3; Figs. 4a and 5a), which suggests an additional DOM source from within the estuaries (discussed further in Sect. 5.3). For West Falmouth Harbor, end-members of the conservative mixing model had $\delta^{13}C$ values of −23.0 and −26.1 ‰. The observed $\delta^{13}C$ data however, ranged from −19.7 to −26.1 ‰, six of which were more ^{13}C-enriched samples than the modeled range. Spatial representation of $\delta^{13}C$ values at West Falmouth Harbor (Fig. 4b) show ^{13}C-depleted samples in the northeastern corner of the harbor, the location of a freshwater culvert discharging groundwater (Ganju, 2011). For Barnegat Bay, end-members of the conservative mixing model had $\delta^{13}C$ values of −22.1 and −26.7 ‰. The observed $\delta^{13}C$ data ranged from −20.8 to −26.7 ‰, four of which were more ^{13}C-enriched than the modeled range. The two points from North Barnegat Bay falling well above the model (Fig. 5a) correspond to sites BB04 and BB09. The two points from South Barnegat Bay falling well above the model correspond to sites BB12 and BB14. These ^{13}C-enriched samples from Barnegat were all taken from areas near significant stretches of marsh along the western edge of Barnegat Bay. Spatial representation of $\delta^{13}C$ values at Barnegat Bay (Fig. 5b) shows significantly less negative $\delta^{13}C$ values in South Barnegat Bay compared to North Barnegat Bay. This indicates more ^{13}C-enriched samples from South Barnegat Bay.

BGD
12, 7301–7333, 2015

4.5 Comparison of isotopic signature and fDOM-CDOM absorption ratio

Comparison of the isotopic and optical analyses suggests a relationship between $\delta^{13}C$ signature and fDOM-CDOM absorption ratio (Fig. 6). For both West Falmouth Harbor and Barnegat Bay, the more ^{13}C-enriched samples also had a higher absorption coefficient per unit fluorescence. This trend is highlighted by the extremes of the dataset, with the most ^{13}C-enriched sample (WF02) displaying the highest fDOM-CDOM absorption ratio, and the least ^{13}C-enriched sample (BB01) displaying the lowest fDOM-CDOM absorption ratio. Furthermore, West Falmouth Harbor samples had both higher fDOM-CDOM absorption ratios (−0.032, natural log scale, average) and ^{13}C enrichment ($\delta^{13}C$ average of −22.4 ‰) as compared to Barnegat Bay (−1.75 and −23.4 ‰, respectively).

5 Discussion

5.1 Spectral slope ranges

At Barnegat Bay and Chincoteague Bay, the range of calculated spectral slopes was quite small (Table 2). At West Falmouth Harbor, however, there was significantly more variability in spectral slope. This is likely due to a combination of several factors. (1) Absorbance measurements via spectrophotometer were taken only from 340–440 nm at West Falmouth Harbor, as opposed to 340–720 nm at Barnegat Bay and Chincoteague Bay. Along with the discarding of non-positive absorbance measurements (see Sect. 3.2), this led to a small number of data points to be plotted for spectral slope calculation at certain West Falmouth Harbor sites. In fact, no spectral slope is reported for site WF01 (Table 2) because only two positive absorbance values were measured for this site. (2) The relatively low DOC concentrations from West Falmouth Harbor contributed to more instrumental variability in spectral slope values at this estuary. Significantly lower fDOM and absorbance measurements were recorded at West

BGD
12, 7301–7333, 2015

Falmouth Harbor compared to Barnegat Bay and Chincoteague Bay (Table 2). (3) West Falmouth Harbor is a relatively dynamic system with multiple freshwater point sources and unique mixing characteristics (Ganju et al., 2012). Considering that DOM source is known to affect its optical properties (Helms et al., 2008; De Souza Sierra et al., 1994) some of the variability in spectral slopes observed at West Falmouth Harbor may be attributable to the physical complexity and short residence time of the estuary. More specifically, previous studies have shown that DOM comprised of primarily fulvic acids has larger spectral slopes than DOM comprised of primarily humic acids (Carder et al., 1989). Considering the complexity of point sources at West Falmouth Harbor, variable organic matter composition and spectral slope is not surprising.

5.2 Variability in fDOM–salinity relationship

The inverse relationship between fDOM and salinity observed for these three estuaries is consistent with previous studies of similar waters (Clark et al., 2002; Green and Blough, 1994). The slope of this inverse relationship varied between and within estuaries. This is due to differences in organic matter composition and fluorescence between the freshwater sources (Stedmon et al., 2003; Parlanti et al., 2000). It is noteworthy that South Barnegat Bay and Chincoteague Bay display a very similar fDOM–salinity relationship, while South Barnegat Bay and North Barnegat Bay show a divergent relationship. South Barnegat Bay and Chincoteague Bay also have geographic and land use similarities with less development and extensive *Spartina alterniflora*-dominated marshes (Wieben and Baker, 2009; Olsen and Mahoney, 2001; Keefe and Boynton, 1973), whereas North Barnegat Bay is much more developed (Wieben and Baker, 2009). Furthermore, North and South Barnegat Bay appear to have different organic matter sources (determined via isotope analysis; see Sect. 5.3). This information considered together supports the idea of differing organic matter sources due to various inputs affecting fluorescence properties. As for the variability seen within West Falmouth Harbor, this is again likely attributable to the relatively low fluorescence signals

BGD
12, 7301–7333, 2015

observed throughout the estuary, along with the variety of freshwater inputs to this complex system.

5.3 Role of additional end-member in isotope mixing

The disparity between observed $\delta^{13}C$ values and those predicted by conservative mixing models (Figs. 4a and 5a) suggest an additional DOM source within the estuaries. Previous studies of DOC in East Coast estuaries have suggested a marine end-member $\delta^{13}C$ value of −24 to −22 ‰, and a freshwater end-member $\delta^{13}C$ of −28 to −26 ‰ (Peterson et al., 1994). Observed values falling above the mixing model and approaching much more ^{13}C-enriched values than the defined marine end-member is likely due to the influence of DOC from *Spartina* spp. cordgrass in nearby salt marshes. Analysis of DOC *Spartina* spp. by past studies has indicated a $\delta^{13}C$ signature of about −16.4 to −11.7 ‰ (Komada et al., 2012; Chmura and Aharon, 1995). The tendency of values from this study towards this ^{13}C-enriched signature, in combination with knowledge of *Spartina* coverage around the sites differing from conservative mixing models, suggests a DOM source derived from *Spartina* cordgrass. The influence of this end-member is particularly notable in South Barnegat Bay (specifically sites BB12 and BB14), where *Spartina* coverage is extensive (Olsen and Mahoney, 2001), and the $\delta^{13}C$ of the DOC is −21.6 and −20.9 ‰ for BB12 and BB14, respectively. Although *Spartina* coverage in North Barnegat Bay is not as extensive as in South Barnegat Bay, the sites with DOC $\delta^{13}C$ values that are more enriched than the conservative mixing model for North Barnegat Bay (BB04 and BB09) were taken from inland sampling locations, specifically the north bank of the lower Toms River and Reedy Creek, where stands of *Spartina* are present.

However, the observed ^{13}C-enrichment could also be attributed to *Zostera* eelgrass, which has been shown to exhibit a ^{13}C-enriched signature (Hemminga and Mateo, 1996). For this reason, the aforementioned samples falling well above the conservative mixing models cannot necessarily be considered a result of *Spartina* influence. However, a comparison of site locations to known seagrass and *Spartina* wetland coverage

BGD
12, 7301–7333, 2015

can yield some indication of the most likely source of ^{13}C-enriched DOC. Seagrass coverage maps (Lathrop and Haag, 2011) and maps of estuarine intertidal wetland coverage (U.S. Fish & Wildlife Service, 2015) for Barnegat Bay show intertidal wetland coverage and no seagrass coverage for sites BB09, BB12, and BB14. Site BB04 is characterized by neither coverage, but its inland location places it much closer to known intertidal wetland coverage (U.S. Fish & Wildlife Service, 2015). This geographic comparison indicates *Spartina* as the more likely additional end-member at Barnegat Bay, though *Zostera* influence is still possible.

For West Falmouth Harbor, sites falling well above the conservative mixing model (WF02, WF03, WF04, WF05, WF07, WF11) were compared to known seagrass (Del Barrio et al., 2014) and intertidal wetland (U.S. Fish & Wildlife Service, 2015) coverage for West Falmouth Harbor. For sites WF03, WF05, WF07, and WF11, there is known intertidal wetland coverage and no known *Zostera* coverage. For site WF02, there is both intertidal wetland coverage and *Zostera* coverage, whereas WF04 corresponds to neither *Spartina* nor *Zostera*. This comparison yields a less clear picture of DOC sources, but this is to be expected considering the aforementioned complexity of surrounding land uses, potential DOC inputs, and limited mixing at West Falmouth Harbor.

5.4 Variability in fDOM-CDOM absorption relationship

The significant variability within a somewhat consistent overall trend between fDOM and absorption by CDOM in these estuaries was expected based on the results of previous studies (Hoge et al., 1993; Del Castillo et al., 1999; Clark et al., 2004). However, the variability in this study can be explained in part by the differing DOC sources within the estuaries. In this study, ^{13}C-enriched DOC sources correspond to a higher absorption coefficient per unit fluorescence (Fig. 6). This assertion is supported by the findings of Tzortziou et al. (2008), which suggested that marsh-exported DOC has a lower fluorescence per unit absorbance as compared to humic DOC (associated with a freshwater source). For our study, ^{13}C-enriched DOC (likely *Spartina* source) was as-

BGD
12, 7301–7333, 2015

sociated with a lower fluorescence per unit absorbance. ^{13}C-depleted DOC (terrestrial source) was associated with a higher fluorescence per unit absorbance. While other studies have focused on differences in the fluorescence–absorbance relationship as a function of molecular weight (Belzile and Guo, 2006; Stewart and Wetzel, 1980), the combination of CDOM optical and isotopic analyses presented here provide a more definitive connection between CDOM source and optical characteristics, as suggested by Tzortziou et al. (2008).

5.5 Ramifications for light attenuation modeling

The variability of fDOM optical properties between and within estuaries has important consequences for light attenuation models. Continuous estimates of light attenuation are possible with continuous proxy measurements of turbidity (for sediment), chlorophyll *a* fluorescence, and fDOM (Gallegos et al., 2011), but Ganju et al. (2014) found that light models can be highly sensitive to the fDOM-CDOM relationship, specifically in Barnegat Bay. We applied the light model of Gallegos et al. (2011) to the individual measurements of turbidity, chlorophyll *a* fluorescence, and fDOM collected in this study. We explored two cases to calculate light attenuation: (1) use of the individual point fDOM-CDOM ratio and spectral slope from measurements; and (2) use of an estuary-wide average fDOM-CDOM ratio and spectral slope (model parameters related to sediment particles and chlorophyll were held constant to values reported in Ganju et al., 2014). Variation in the DOM properties led to average light attenuation errors ranging from 11 to 33 % (Table 4), with individual site errors over 200 % at sites with the highest deviation from the estuary mean (site BB01, at the landward end of Barnegat Bay). This suggests that constraining optical properties of the DOM pool is critical for light modeling, and that high variability within an estuary may confound use of spatially constant parameters.

BGD
12, 7301–7333, 2015

6 Conclusions

The results of this study show that the fDOM-CDOM absorption relationship is variable both between and within West Falmouth Harbor, Barnegat Bay, and Chincoteague Bay, and depends upon DOM source. DOM that is ^{13}C-enriched (higher δ^{13}C values) also has a higher absorption coefficient per unit fluorescence. Additionally, fDOM–salinity relationship is variable between and within these estuaries. The exception here is the lack of variability in these relationships within Chincoteague Bay. Future work in relation to this study might involve a stable carbon isotope analysis at Chincoteague Bay similar to the analysis carried out here for West Falmouth Harbor and Barnegat Bay. Results of such an analysis could further elucidate the effects of DOM source on the fDOM-CDOM absorption ratio. Finally, spectral slopes for use in light models are consistent between and within Barnegat and Chincoteague Bays, with more variability observed at West Falmouth Harbor. In combination, these results will help to inform future monitoring of light attenuation, and therefore potential seagrass viability in shallow estuaries.

Author contributions. W. K. Oestreich executed the sampling strategy and analyzed data. N. K. Ganju and J. W. Pohlman designed the experiment and assisted in data interpretation. S. E. Suttles assisted in designing and executing the sampling strategy. All authors contributed to the drafting of the manuscript.

Acknowledgements. Funding was provided by the Woods Hole Oceanographic Institution Summer Student Fellowship Program and the USGS Coastal and Marine Geology Program. Thanks to Brian Bergamaschi of the U.S. Geological Survey California Water Science Center for input on fDOM corrections. Thanks to the Rutgers University Marine Field Station, in particular Tom Malatesta and Roland Hagan, for field support at Barnegat Bay. Thanks also to Nicholas Nidzieko of the University of Maryland Horn Point Laboratory for field support at Chincoteague Bay. Patrick Dickhudt and Wally Brooks provided assistance with instrument preparation and running of stable carbon isotope analysis samples, respectively. The USGS–WHOI Dissolved Carbon Isotope Lab (DCIL) assisted in the isotope analysis. Any use of trade, firm, or product names is for descriptive purposes only and does not imply endorsement by the US Government.

BGD
12, 7301–7333, 2015

References

Allen, T. R., Tolvanen, H. T., Oertel, G. F., and McLeod, G. M.: Spatial characterization of environmental gradients in a coastal lagoon, Chincoteague Bay, Estuar. Coast., 30, 959–977, 2007.

Baker, A.: Thermal fluorescence quenching properties of dissolved organic matter, Water Res., 39, 4405–4412, 2005.

Belzile, C. and Guo, L.: Optical properties of low molecular weight and colloidal organic matter: application of the ultrafiltration permeation model to DOM absorption and fluorescence, Mar. Chem., 98, 183–196, 2006.

Bricaud, A., Morel, A., and Prieur, L.: Absorption by dissolved organic matter of the sea (yellow substance) in the UV and visible domains, Limnol. Oceanogr., 26, 43–53, 1981.

Bricker, S. B., Clement, C. G., Pirhalla, D. E., Orlando, S. P., and Farrow, D. R. G.: National Estuarine Eutrophication Assessment: Effects of Nutrient Enrichment in the Nation's Esuaries, NOAA, National Ocean Service, Special Projects Office and the National Centers for Coastal Ocean Science, Silver Spring, MD, 71 pp., 1999.

Buchsbaum, R. and Valiela, I.: Variability in the chemistry of estuarine plants and its effect on feeding by Canada geese, Oecologia, 73, 146–153, 1987.

Burkholder, J. M., Tomasko, D. A., and Touchette, B. W.: Seagrasses and eutrophication, J. Exp. Mar. Biol. Ecol., 350, 46–72, 2007.

Callahan, J., Dai, M., Chen, R. F., Li, X., Lu, Z., and Huang, W.: Distribution of dissolved organic matter in the Pearl River Estuary, China, Mar. Chem., 89, 211–224, 2004.

Chen, C., Shi, P., Yin, K., Pan, Z., Zhan, H., and Hu, Z.: Absorption coefficient of yellow substance in the Pearl River estuary, Proc. SPIE 4892, P. Soc. Photo-Opt. Ins., 215–221, 2003.

Chmura, G. L. and Aharon, P.: Stable carbon isotope signatures of sedimentary carbon in coastal wetlands as indicators of salinity regime, J. Coast. Res., 11, 124–135, 1995.

Clark, C. D., Jimenez-Morais, J., Jones II, G., Zanardi-Lombardo, E., Moore, C. A., and Zika, R. G.: A time-resolved fluorescence study of dissolved organic matter in a riverine to marine transition zone, Mar. Chem., 78, 121–135, 2002.

Clark, C. D., Hiscock, W. T., Millero, F. J., Hitchcock, G., Brand, L., Miller, W. L., Ziolkowski, L., Chen, R. F., and Zika, R. G.: CDOM distribution and CO_2 production on the Southwest Florida Shelf, Mar. Chem., 89, 145–167, 2004.

BGD
12, 7301–7333, 2015

De Souza Sierra, M. M., Donard, O. F. X., Lamotte, M., Belin, C., and Ewald, M.: Fluorescence spectroscopy of coastal and marine waters, Mar. Chem., 47, 127–144, 1994.
Defne, Z. and Ganju, N. K.: Quantifying the residence time and flushing characteristics of a shallow, back-barrier estuary: application of hydrodynamic and particle tracking models, Estuar. Coast., 1–16, doi:10.1007/s12237-014-9885-3, 2014.
Del Barrio, P., Ganju, N. K., Aretxabaleta, A. L., Hayn, M., Garcia, A., and Howarth, R. W.: Modeling future scenarios of light attenuation and potential seagrass success in a eutrophic estuary, Estuar. Coast. Shelf S, 149, 13–23, 2014.
Del Castillo, C. E., Coble, P. G., Morell, J. M., Lopez, J. M., and Corredor, J. E.: Analysis of optical properties of the Orinoco River plume by absorption and fluorescence spectroscopy, Mar. Chem., 66, 35–51, 1999.
Downing, B. D., Pellerin, B. A., Bergamaschi, B. A., Saraceno, J. F., and Kraus, T. E. C.: Seeing the light: the effects of particles, dissolved materials, and temperature on in situ measurements of DOM fluorescence in rivers and streams, Limnol. Oceanogr.-Meth., 10, 767–775, 2012.
Ehlers, A., Worm, B., and Reusch, T. B. H.: Importance of genetic diversity in eelgrass *Zostera marina* for its resilience to global warming, Mar. Ecol.-Prog. Ser., 355, 1–7, 2008.
Gallegos, C. L., Werdell, P. J., and McClain, C. R.: Long-term changes in light scattering in Chesapeake Bay inferred from Secchi depth, light attenuation, and remote sensing measurements, J. Geophys. Res., 116, C00H08, doi:10.1029/2011JC007160, 2011.
Ganju, N. K.: A novel approach for direct estimation of fresh groundwater discharge to an estuary, Geophys. Res. Lett., 38, L11402, doi:10.1029/2011GL047718, 2011.
Ganju, N. K., Hayn, M., Chen, S.-N., Howarth, R. W., Dickhudt, P. J., Aretxabaleta, A. L., and Marino, R.: Tidal and groundwater fluxes to a shallow, microtidal estuary: constraining inputs through field observations and hydrodynamic modeling, Estuar. Coast., 35, 1285–1298, doi:10.1007/s12237-012-9515-x, 2012.
Ganju, N. K., Miselis, J. L., and Aretxabaleta, A. L.: Physical and biogeochemical controls on light attenuation in a eutrophic, back-barrier estuary, Biogeosciences, 11, 7193–7205, doi:10.5194/bg-11-7193-2014, 2014.
Green, S. A. and Blough, N. V.: Optical absorption and fluorescence properties of chromophoric dissolved organic matter in natural waters, Limnol. Oceanogr., 39, 1903–1916, 1994.
Harvey, G. R., Boran, D. A., Chesal, L. A., and Tokar, J. M.: The structure of marine fulvic and humic acids, Mar. Chem., 12, 119–132, 1983.

BGD
12, 7301–7333, 2015

Hauxwell, J., Cebrián, J., Valiela, I.: Eelgrass *Zostera marina* loss in temperate estuaries: relationship to land-derived nitrogen loads and effect of light limitation imposed by algae, Mar. Ecol.-Prog. Ser., 247, 59–73, 2003.
Hayn, M., Howarth, R., Marino, R., Ganju, N., Berg, P., Foreman, K., Giblin, A., and McGlathery, K.: Exchange of nitrogen and phosphorus between a shallow lagoon and coastal waters, Estuar. Coast., 37, 63–73, 2014.
Heck, K. L., Able, K. W., Roman, T. C., and Fahay, M. P.: Composition, abundance, biomass, and production of macrofauna in a New England estuary: comparisons among eelgrass meadows and other nursery habitats, Estuaries, 18, 379–389, 1995.
Helms, J. R., Stubbins, A., Ritchie, J. D., Minor, E. C., Kieber, D. J., and Mopper, K.: Absorption spectral slopes and slope ratios as indicators of molecular weight, source, and photobleaching of chromophoric dissolved organic matter, Limnol. Oceanogr., 53, 955–969, 2008.
Hemminga, M. A. and Mateo, M. A.: Stable carbon isotopes in seagrasses: variability in ratios and use in ecological studies, Mar. Ecol.-Prog. Ser., 140, 285–298, 1996.
Hoge, F. E., Vodacek, A., and Blough, N. V.: Inherent optical properties of the ocean: retrieval of the absorption coefficient of chromophoric dissolved organic matter from fluorescence measurements, Limnol. Oceanogr., 38, 1394–1402, 1993.
Kaldy, J. E., Cifuentes, L. A., and Brock, D.: Using stable isotope analyses to assess carbon dynamics in a shallow subtropical estuary, Estuaries, 28, 86–95, 2005.
Keefe, C. W. and Boynton, W. R.: Standing crop of salt marshes surrounding Chincoteague Bay, Maryland-Virginia, Chesapeake Sci., 14, 117–123, 1973.
Keith, D. J., Yoder, J. A., and Freeman, S. A.: Spatial and temporal distribution of coloured dissolved organic matter (CDOM) in Narragansett Bay, Rhode Island: implications for phytoplankton in coastal waters, Estuar. Coast. Shelf S, 55, 705–717, 2002.
Kennish, M. J., Fertig, B. M., and Sakowicz, G. P.: Benthic macroalgal blooms as an indicator of system eutrophy in the Barnegat Bay–Little Egg Harbor estuary, Bull. N. J. Acad. Sci., 56, 1–5, 2011.
Kennish, M. J., Fertig, B. M., and Sakowicz, G. P.: In situ surveys of seagrass habitat in the northern segment of the Barnegat bay–Little Egg Harbor estuary, available at: http://bbp.ocean.edu/Reports/2011%20Northern%20seagrass%20survey.pdf, 2013.
Kirk, J. T. O.: Light and Photosynthesis in Aquatic Ecosystems, Cambridge University Press, Cambridge and New York, 1994.

BGD
12, 7301–7333, 2015

Komada, T., Polly, J. A., and Johnson, L.: Transformations of carbon in anoxic marine sediments: implications from $\Delta^{14}C$ and $\delta^{13}C$ signatures, Limnol. Oceanogr., 57, 567–581, 2012.
Lalonde, K., Middlestead, P., and Gelinas, Y.: Automation of $^{13}C/^{12}C$ ratio measurement for freshwater and seawater DOC using high temperature combustion, Limnol. Oceanogr.-Meth., 12, 816–829, 2014.
McGranahan, G., Balk, D., Anderson, B.: The rising tide: assessing the risks of climate change and human settlements in low elevation coastal zones, Environ. Urban, 19, 17–37, 2007.
Olsen, P. S. and Mahoney, J. B.: Phytoplankton in the Barnegat Bay–Little Egg Harbor estuarine system: species composition and picoplankton bloom development, J. Coast. Res., 32, 115–143, 2001.
Parlanti, E., Worz, K., Geoffroy, L., and Lamotte, M.: Dissolved organic matter fluorescence spectroscopy as a tool to estimate biological activity in a coastal zone submitted to anthropogenic inputs, Org. Geochem., 31, 1765–1781, 2000.
Peterson, B. J., Fry, B., Hullar, M., Saupe, S., and Wright, R.: The distribution and stable carbon isotopic composition of dissolved organic carbon in estuaries, Estuaries, 17, 111–121, 1994.
Raymond, P. A. and Bauer, J. E.: DOC cycling in a temperate estuary: a mass balance approach using natural ^{14}C and ^{13}C isotopes, Limnol. Oceanogr., 46, 655–667, 2001.
Stedmon, C. A., Markager, S., and Bro, R.: Tracing dissolved organic matter in aquatic environments using a new approach to fluorescence spectroscopy, Mar. Chem., 82, 239–254, 2003.
Stewart, A. J. and Wetzel, R. G.: Fluorescence: absorbance ratios – a molecular-weight tracer of dissolved organic matter, Limnol. Oceanogr., 25, 559–564, 1980.
Tzortziou, M., Neale, P. J., Osburn, C. L., Megonigal, J. P., Nagamitzu, M., and Rudolf, J.: Tidal marshes as a source of optically and chemically distinctive colored dissolved organic matter in the Chesapeake Bay, Limnol. Oceanogr., 53, 148–159, 2008.
United States Environmental Protection Agency: National estuary program coastal condition report, Chap. 3: Northest national estuary program coastal condition, Barnegat Bay National Estuary Program, available at: http://www.epa.gov/owow/oceans/nepccr/index.html, 2007.
United States Fish and Wildlife Service National Wetlands Inventory, Ecological Services: Wetlands Mapper, available at: http://www.fws.gov/wetlands/data/mapper.HTML, 2015.
Wazniak, C., Hall, M., Cain, C., Wilson, D., Jesien, R., Thomas, J., Carruthers, C., and Dennison, W.: State of the Maryland coastal bays, Maryland Department of Natural Resources, Maryland Coastal Bays Program, and University of Maryland Center for Environ-

BGD
12, 7301–7333, 2015

mental Science, Integration, and Application Network, Annapolis, MD, available at: http://mdcoastalbays.org/files/pdfs_pdf/StateoftheBays2004.pdf, 2004.
Wieben, C. M. and Baker, R. J.: Contributions of nitrogen to the Barnegat Bay–Little Egg Harbor Estuary: updated loading estimates, 19 p., Chapter prepared for the Barnegat Bay Partnership State of the Bay Technical Report, 2009.

BGD
12, 7301–7333, 2015

Table 1. Sampling sites and procedures.

Estuary	No. of sites	Site ID's	Isotope Analysis (Y/N)	Date
West Falmouth Harbor, MA	13	WF01–WF13	Yes	25 Jun 2014
Barnegat Bay, NJ	16	BB01–BB16	Yes	14–15 Jul 2014
North Barnegat Bay (BB-N)	8	BB01–BB04; BB08–BB11	Yes	14–15 Jul 2014
South Barnegat Bay (BB-S)	8	BB05–BB07; BB12–BB16	Yes	14–15 Jul 2014
Chincoteague Bay, MD/VA	10	CB01–CB10	No	17 Jul 2014

BGD
12, 7301–7333, 2015

Table 2. Optical characteristics of all samples.

Site	Lat, Long	Salinity (psu)	a(340 nm)	fDOM (QSU)	$\frac{a(340\text{ nm})}{\text{fDOM}}$	S
West Falmouth Harbor						
WF01	41.606, −70.652	31.35	0.921	1.638	0.562	[a]
WF02	41.605, −70.645	31.28	2.672	0.631	4.232	0.044
WF03	41.598, −70.647	31.17	4.284	5.014	0.854	0.022
WF04	41.604, −70.639	28.29	3.316	1.904	1.742	0.022
WF05	41.607, −70.636	15.94	2.810	2.184	1.286	0.049
WF06	41.616, −70.632	0.13	2.349	5.363	0.438	0.026
WF07	41.596, −70.639	26.65	4.007	5.247	0.764	0.026
WF08	41.598, −70.649	30.11	3.362	2.993	1.123	0.026
WF09	41.606, −70.652	31.20	3.915	2.317	1.690	0.013
WF10	41.605, −70.645	30.34	3.316	2.862	1.159	0.029
WF11	41.599, −70.643	29.26	3.685	6.317	0.583	0.019
WF12	41.604, −70.639	25.14	3.501	5.118	0.684	0.025
WF13	41.609, −70.637	11.30	5.067	10.205	0.497	0.014
Barnegat Bay						
BB01	40.066, −74.131	3.41	0.967	62.919	0.015	0.012
BB02	40.058, −74.066	20.64	6.310	34.585	0.183	0.012
BB03	39.949, −74.163	10.61	8.199	52.835	0.155	0.014
BB04	39.951, −74.113	20.55	6.356	36.176	0.176	0.018
BB05	39.821, −74.203	26.88	3.685	21.469	0.172	0.012
BB06	39.797, −74.181	28.50	3.132	17.081	0.183	0.012
BB07	39.577, −74.331	27.50	4.790	27.316	0.175	0.012
BB08	39.964, −74.097	20.98	6.218	31.522	0.197	0.018
BB09	40.030, −74.080	17.82	11.193	68.842	0.163	0.015
BB10	40.053, −74.058	19.92	6.587	34.058	0.193	0.013
BB11	40.044, −74.056	19.66	6.725	32.600	0.206	0.013
BB12	39.643, −74.245	27.99	6.034	32.741	0.184	0.011

BGD
12, 7301–7333, 2015

Table 2. Continued

Site	Lat, Long	Salinity (psu)	a(340 nm)	fDOM (QSU)	$\frac{a(340\,nm)}{fDOM}$	S
BB13	39.632, −74.219	30.08	2.625	12.061	0.218	0.010
BB14	39.637, −74.262	24.17	14.463	84.399	0.171	0.015
BB15	39.604, −74.260	29.62	14.970	16.499	0.907	0.014
BB16	39.509, −74.325	29.69	3.270	15.308	0.214	0.013
Chincoteague Bay						
CB01	37.980, −75.397	31.63	1.842	11.152	0.165	0.006
CB02	37.975, −75.345	31.42	1.889	11.501	0.164	0.015
CB03	38.239, −75.214	25.88	8.383	49.485	0.169	0.014
CB04	38.010, −75.309	31.37	2.533	15.003	0.169	0.019
CB05	38.012, −75.308	31.37	2.718	16.177	0.168	0.020
CB06	38.149, −75.238	29.50	3.823	22.307	0.171	0.016
CB07	38.091, −75.283	31.39	3.316	20.912	0.159	0.014
CB08	38.090, −75.252	31.85	3.132	18.626	0.168	0.016
CB09	38.159, −75.212	30.12	3.408	21.772	0.157	0.010
CB10	38.098, −75.250	29.40	3.823	24.551	0.156	0.013

[a] No spectral slope calculated due to only two positive absorbance measurements at this site.

BGD
12, 7301–7333, 2015

Table 3. Stable carbon isotope analysis data for samples from West Falmouth Harbor and Barnegat Bay.

	Sample	DOC Conc (ppm)	µM DOC	$\delta^{13}C/^{12}C$ (‰)	$\delta^{13}C_{corr}$ (‰)
	CONTROL	−0.02	−1.53	−21.9	18.0
West Falmouth Harbor	WF01	1.59	127.58	−23.1	−23.8
	WF02	1.29	107.27	−19.7	−19.8
	WF03	0.86	71.84	−20.8	−21.3
	WF04	1.68	133.93	−21.9	−22.4
	WF05	1.35	113.06	−22.5	−23.2
	WF06	0.73	60.67	−26.1	−28.7
	WF07	1.95	161.92	−21.4	−21.7
	WF08	2.40	199.71	−22.6	−23.0
	WF09	2.12	175.82	−22.8	−23.3
	WF10	2.07	172.46	−22.6	−23.1
	WF11	1.87	155.63	−21.6	−21.9
	WF12	1.74	145.06	−22.8	−23.4
	WF13	2.09	174.74	−23.6	−24.2
Barnegat Bay	BB01	5.36	446.33	−26.7	−27.1
	BB02	5.04	420.15	−24.7	−25.0
	BB03	4.87	405.19	−25.6	−26.0
	BB04	4.06	338.07	−23.7	−24.0
	BB05	3.00	249.74	−22.6	−23.0
	BB06	3.36	280.03	−23.0	−23.4
	BB07	4.15	361.45	−23.0	−23.2
	BB08	4.96	412.62	−24.2	−24.5
	BB09	6.34	527.28	−23.8	−24.0
	BB10	4.91	408.48	−24.4	−24.7
	BB11	5.36	445.79	−24.4	−24.7
	BB12	3.93	327.40	−21.5	−21.6
	BB13	2.65	220.15	−22.1	−22.4
	BB14	6.99	581.80	−20.8	−20.9
	BB15	2.78	231.45	−22.4	−22.7
	BB16	2.50	207.87	−22.2	−22.6

BGD
12, 7301–7333, 2015

Table 4. Light attenuation model parameters and ensuing errors arising from usage of estuary-wide mean values. Note reduced number of significant figures for reporting of spectral slope as compared to Table 2.

Estuary	Mean fDOM/CDOM ratio (range)	Mean spectral slope (range)	Mean light attenuation error (range)
West Falmouth Harbor, MA	1.2 (0.50–4.3)	0.03 (0.01–0.05)	15 % (0–52 %)
Barnegat Bay, NJ	0.23 (0.01–0.96)	0.01 (0.01–0.02)	33 % (0–220 %)
Chincoteague Bay, MD, VA	0.17 (0.16–0.19)	0.01 (0.01–0.02)	11 % (0.01–28 %)

BGD
12, 7301–7333, 2015

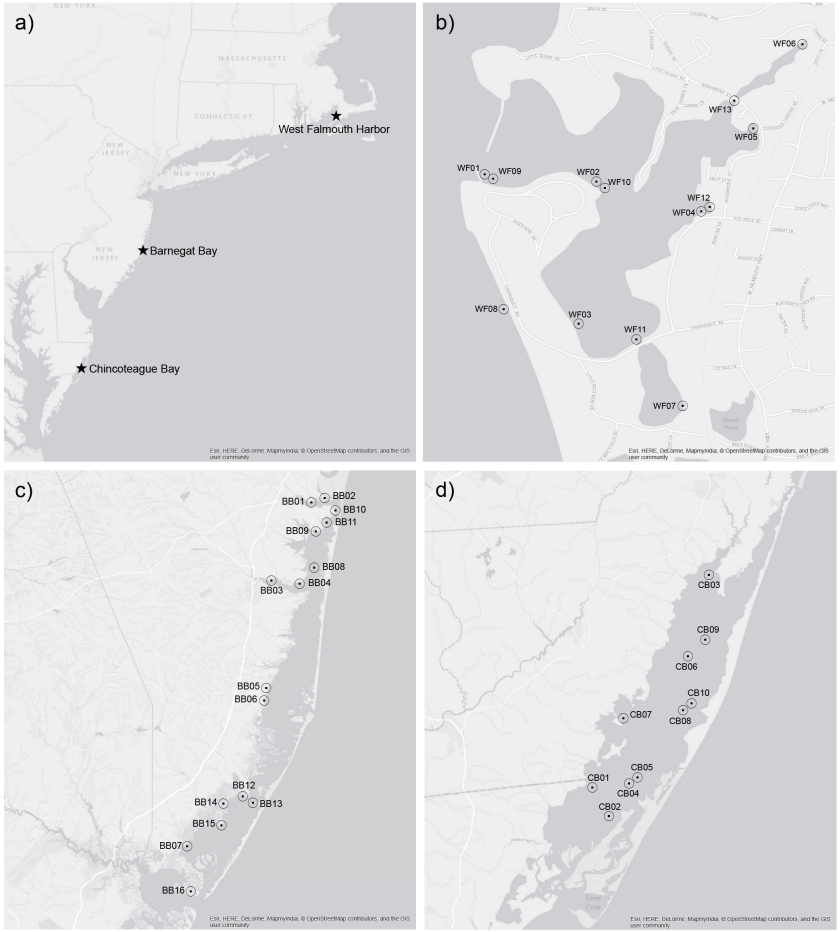

Figure 1. (a) Location of estuaries on the US Atlantic Coast. Study sites within **(b)** West Falmouth Harbor; **(c)** Barnegat Bay; **(d)** Chincoteague Bay.

BGD
12, 7301–7333, 2015

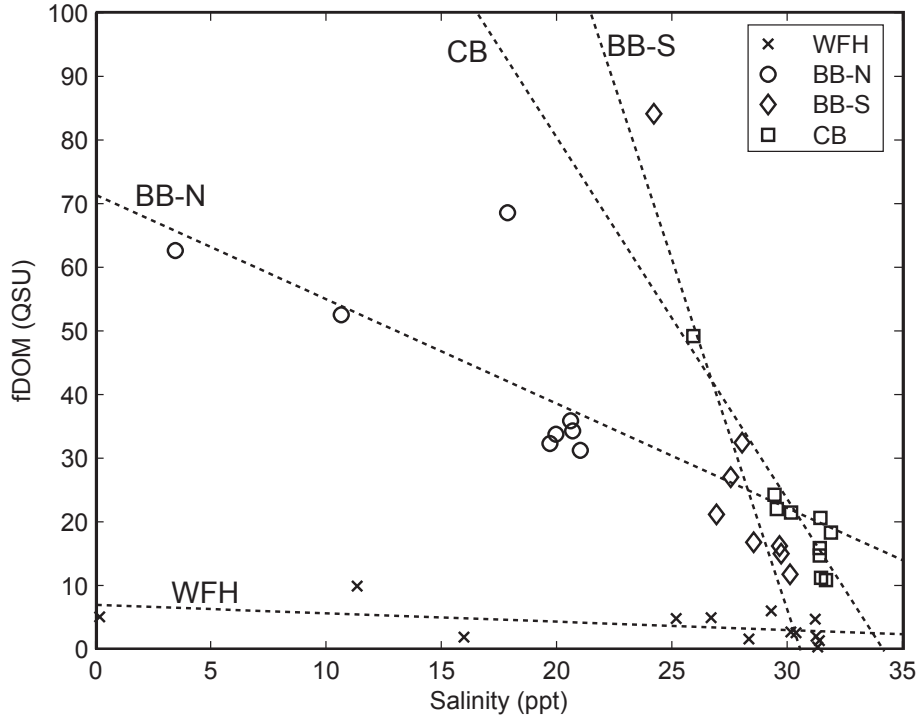

Figure 2. Fluorescence measurement vs. salinity for all sample sites at West Falmouth Harbor (WFH), North Barnegat Bay (BB-N), South Barnegat Bay (BB-S), and Chincoteague Bay (CB).

BGD
12, 7301–7333, 2015

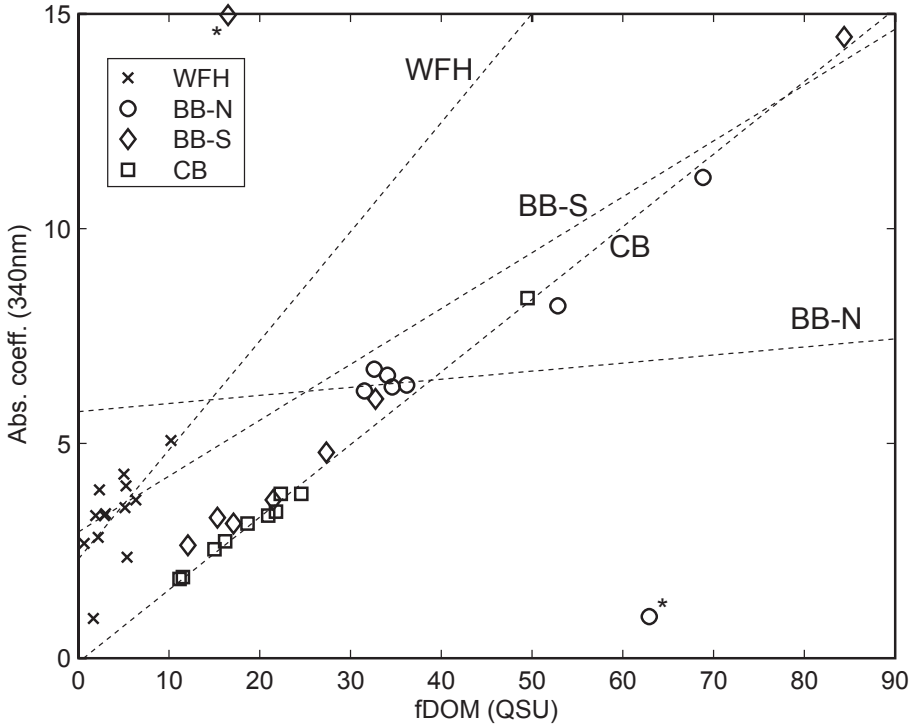

Figure 3. Absorption coefficient at 340 nm vs. fluorescence measurement for all sampling sites at West Falmouth Harbor (WFH), North Barnegat Bay (BB-N), South Barnegat Bay (BB-S), and Chincoteague Bay (CB).

BGD
12, 7301–7333, 2015

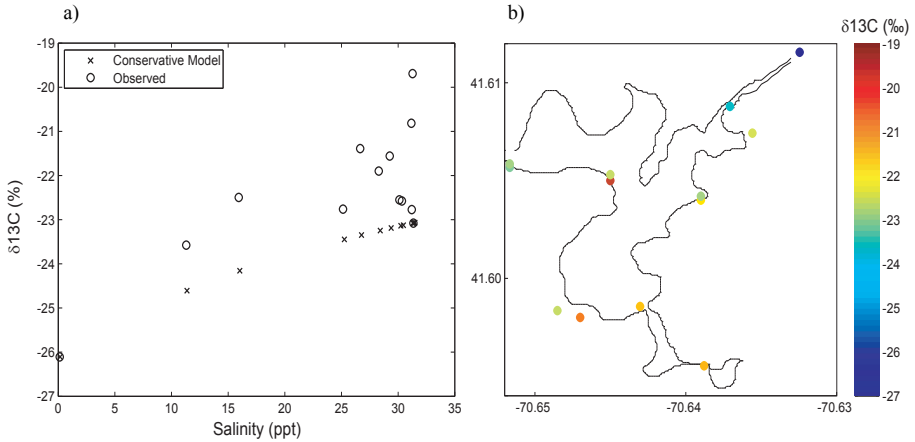

Figure 4. (a) Conservative mixing model of $\delta^{13}C$ vs. salinity for West Falmouth Harbor. Both conservative model and observed isotopic signatures represented. **(b)** Spatial plot of isotopic signatures measured at West Falmouth Harbor.

BGD
12, 7301–7333, 2015

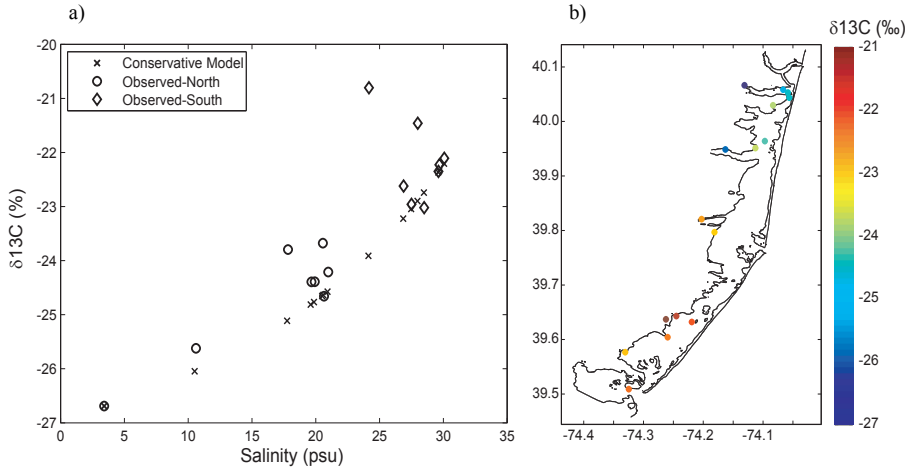

Figure 5. (a) Conservative mixing model of $\delta^{13}C$ vs. salinity for Barnegat Bay. Both conservative model and observed isotopic signatures for North Barnegat Bay and South Barnegat Bay represented. **(b)** Spatial plot of isotopic signatures measured at Barnegat Bay.

BGD
12, 7301–7333, 2015

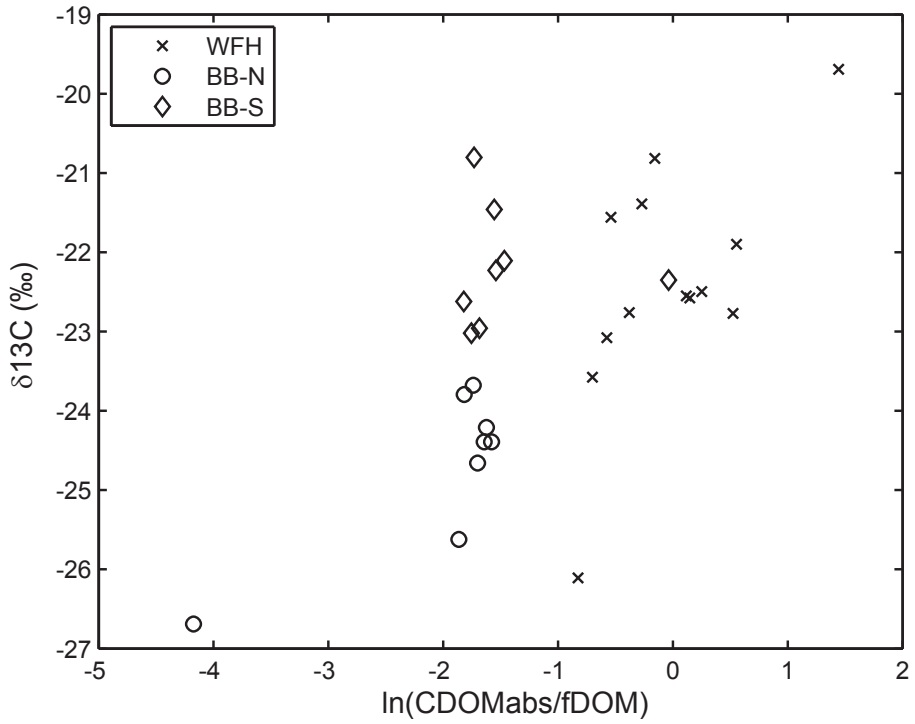

Figure 6. Isotopic signature vs. CDOM absorption coefficient (340 nm) divided by fluorescence for all sites at West Falmouth Harbor (WFH), North Barnegat Bay (BB-N), and South Barnegat Bay (BB-S). Fluorescence per CDOM absorption coefficient presented on natural log scale.

BGD
12, 7301–7333, 2015